DISPERSION ANALYSIS AND ELEMENT-FREE GALERKIN SIMULATIONS OF HIGHER-ORDER STRAIN GRADIENT MODELS

H. Askes[1], A.S.J. Suiker[2] and L.J. Sluys[1]

Koiter Institute Delft / Delft University of Technology, Faculties of Civil Engineering and Geosciences[1] and of Aerospace Engineering[2], P.O. Box 5048, 2600 GA Delft, The Netherlands

Abstract. The role of strain gradients in continuum mechanics has been studied. Distinction is made between stabilizing and destabilizing gradients. A combined model is proposed to investigate the interaction of the two effects. Dispersion analysis and numerical simulations are used to compare the various formats of the model in a qualitative and a quantitative manner. It is shown that a destabilizing second-order gradient has a devastating effect on the numerical response, even if a stabilizing second-order gradient is present. For this class of models only the absence of destabilizing terms guarantees convergent numerical responses.

1. INTRODUCTION

The use of standard continuum material models, in which the stresses are related to the strains, fails when phenomena must be described that occur at a smaller scale of observation. These microstructural processes can be incorporated into the continuum description by addition of higher-order gradients, which results in non-standard continuum models. This class of continuum models is normally denoted as *enhanced continuum models*. Enhanced continuum models have proven to be effective in the simulation of strain localization phenomena, e.g. [1-5]. Furthermore, enhanced models can be used to capture the inhomogeneous granular effects on the wave propagation characteristics [6-8].

Different procedures can be followed to add higher-order gradients to the standard continuum description. For instance, they can be postulated from a phenomenological manner. Alternatively, homogenization of the microstructure can also be used to derive higher-order gradient models. In either case, care must be taken of the effect that the higher-order gradients have on the stability of the model. Indeed, a straightforward inclusion of higher-order gradients may lead to continuum models that behave in an unstable manner [9].

Below, we will focus on higher-order strain gradient models, i.e. higher-order stress gradients will not be considered. Furthermore, restriction is made to second-order gradients. Thus, the stresses are related to the strains as well as to the second-order spatial derivatives of the strains. For clarity's sake only one-dimensional cases are treated. Distinction is made between gradients that have a *stabilizing* effect and gradients that are *destabilizing*. First, the differences between these types of gradients are discussed. Next, a model is treated in which both types of gradients are present. Dispersion analysis is used to study qualitatively the effects of the gradients on the response. These effects are studied quantitatively by means of the Element-Free Galerkin (EFG) method [10,11]. The EFG method is a numerical discretization method that enables a straightforward inclusion of higher-order gradients in the continuum description [12,13]. As such, different higher-order gradient models can easily be compared as regards their numerical linear and nonlinear response. By means of a dispersion analysis and the EFG method it is investigated

---

Corresponding author: H. Askes, e-mail: h.askes@citg.tudelft.nl

whether the divergent effect of the destabilizing gradient terms can be compensated with stabilizing gradient terms. Finally, conclusions are drawn and lines for future investigations are given.

2. SECOND-ORDER STRAIN GRADIENT MODELS

The simplest format in which a second-order strain gradient is added to the constitutive relation reads

$$\sigma = E\left(\varepsilon + c\frac{\partial^2\varepsilon}{\partial x^2}\right), \tag{1}$$

where σ is the stress, ε is the strain, E is Young's modulus and c is a coefficient with the dimension of length squared. By taking $c = 0$ the standard continuum is retrieved. Following the literature, basically two versions of second-order gradient models exist, namely those models where $c = -l^2$ and those where $c = +l^2$. Here, the length scale parameter l is related to the dimension of microstructural quantities such as aggregates [14,15]. The sign of the higher-order coefficient has important implications for the behaviour of the model, as is shown in the sequel.

Energy considerations. The stability of higher-order models is investigated by means of the potential energy density U, which is written as

$$U = \int \sigma d\varepsilon \tag{2}$$

in which we assume an infinite domain for simplicity. When we substitute the general second-gradient constitutive relation (1), integrate the second-order term by parts and carry out the integrations, we obtain

$$U = \frac{1}{2}E\left(\varepsilon^2 - c\left(\frac{\partial\varepsilon}{\partial x}\right)^2\right). \tag{3}$$

In expression (3) terms with a positive sign stabilize the model behaviour, whereas negative signs destabilize the model. Obviously, the standard (zeroth order) term is stabilizing. However, for the higher-order term this depends on the sign of c. Taking $c = -l^2$ results in a stable material model, while $c = +l^2$ leads to a destabilized model. This becomes also manifest in the exact solutions that can be derived for the linear elastic case.

Exact solutions for the linear elastic case. When the general constitutive equation (1) is considered together with the static equilibrium equation $\partial\sigma/\partial x = 0$ (assuming no body forces are present) and the kinematic equation $\varepsilon = \partial u/\partial x$ with u the displacement, the exact solution can be derived as

$$u = A_1 + A_2 x + A_3 \sin\frac{x}{l} + A_4 \cos\frac{x}{l} \tag{4}$$

for the case that $c = +l^2$, and

$$u = B_1 + B_2 x + B_3 \exp\left(-\frac{x}{l}\right) + B_4 \exp\frac{x}{l} \tag{5}$$

for the case $c = -l^2$. In these expressions, A_i and B_i denote constants that have to be solved according to the boundary conditions. The behaviour of the destabilized model differs completely from that of a stabilized model: while the destabilized case leads to a periodic response, the response for the stabilized model is non-periodic. Furthermore, local perturbations lead to strain gradient activity in the *entire* domain for the destabilized case, whereas the exponential character of the stabilized model ensures that local perturbations remain local.

A combined model. In order to study the simultaneous effect of stabilizing and destabilizing second-order strain gradients, a damage model is chosen as

$$\sigma = (1-D)E\left(\varepsilon + c\frac{\partial^2\varepsilon}{\partial x^2}\right) \tag{6}$$

in which D is the damage parameter that ranges from 0 initially to 1 in the final stage. The damage is taken as a function of the strain level as well as of its second gradient in correspondence with the literature [1,2,4]. We assume a simple, linear format according to

$$D = \frac{1}{\kappa_u}\left(\varepsilon + l^2\frac{\partial^2\varepsilon}{\partial x^2}\right), \tag{7}$$

where κ_u is the strain level at which all load carrying capacity is exhausted*. With this linear damage law, for $0<D<0.5$ a *hardening* response is obtained, whereas *softening* takes place for $0.5<D<1$. With this definition of the damage, two strain gradients have entered the constitutive equation. Replacing c in Eq.(6) by $+l^2$ and substituting Eq. (7) yields

---

* Normally, in damage models loading and unloading must be distinguished. However, since we consider only loading this difference can be neglected.

$$\sigma = \left(1 - \frac{\varepsilon + l_s^2 \dfrac{\partial^2 \varepsilon}{\partial x^2}}{\kappa_u}\right) E\left(\varepsilon + l_d^2 \frac{\partial^2 \varepsilon}{\partial x^2}\right),$$ (8)

where the two length scale parameters l have been marked with subscripts s and d. In this model, the negative sign that precedes the l_s^2 gradient term implies that this term is stabilizing. On the other hand, the l_d^2 term is destabilizing as it is preceded by a positive sign, see above.

3. DISPERSION ANALYSIS

The stabilizing and destabilizing second-gradient terms have an important impact on the ability of the material to transform the shape of a passing wave. If the phase velocity varies with the wave number, the shape of the wave is changed and the material is denoted as *dispersive*. The dispersion analysis is started with the one-dimensional equation of motion, in which the body forces are neglected,

$$\rho \ddot{u} = \frac{\partial \sigma}{\partial x},$$ (9)

where ρ is the mass density and a superimposed dot denotes a time derivative. An infinitely long bar is considered with a uniform strain field and a corresponding uniform damage field. Substitution of Eq. (8) then results in

$$\frac{1}{c_u^2} \ddot{u} = (1 - D_0)\left(\frac{\partial^2 u}{\partial x^2} + l_d^2 \frac{\partial^4 u}{\partial x^4}\right) -$$
$$D_0\left(\frac{\partial^2 u}{\partial x^2} + l_s^2 \frac{\partial^4 u}{\partial x^4}\right),$$ (10)

where $c_e = \sqrt{E/\rho}$ is the elastic bar velocity, D_0 is the uniform damage level and it has been used that spatial derivatives of the strain field vanish due to the uniformity of the strain. Loading is assumed to occur through a perturbation of the displacement field $\delta u = \hat{u}\exp(ik(ct - x))$ with $\hat{u}$ the amplitude of the perturbation, k the wave number and c the phase velocity. When this perturbation is substituted into Eq. (10) we obtain the dispersion relation

$$\frac{c^2}{c_e^2} = 1 - 2D_0 - (1 - D_0)l_d^2 k^2 + D_0 l_s^2 k^2.$$ (11)

The phase velocity c (normalized with respect to the elastic bar velocity c_e) is plotted in Fig. 1 as a function of the wave number for different damage levels and for different values of the length scales l_d and l_s. Some combinations lead to cases where all wave numbers have imaginary phase velocities for certain damage levels. For instance, the classical continuum ($l_s = l_d = 0$) only gives real phase velocities for $D_0 \le 0.5$. For the purely destabilized model ($l_s = 0, l_d \ne 0$) damage levels $D_0 > 0.5$ also lead to imaginary phase velocities for all wave numbers, but also for $D_0 < 0.5$ the higher wave numbers have imaginary phase velocities. On the other hand, the purely stabilized model ($l_s = 1, l_d = 0$) has real phase velocities for all damage levels, although for $D_0 > 0.5$ a threshold value for k exists below which the phase velocities are imaginary. When the destabilizing effect and the stabilizing effect are present simultaneously, the response of the model depends on the ratio l_s / l_d. In each case, for lower damage levels the response is dominated by the destabilizing term while the stabilizing term is more important for higher damage levels.

An important difference between the various alternatives concerns with the location of the cut-off value for the wave number, i.e. the wave number for which $c = 0$. This case, which represents the static case, indicates above or below which value k the waves are able to propagate. The wave length that corresponds to this cut-off value k_{crit} is determined as $\lambda_{crit} = 2\pi/k_{crit}$. In Fig. 2 the critical wave lengths are plotted that correspond to the phase velocity curves of Fig. 1. The critical wave length curve of the classical model ($l_s = l_d = 0$) shows that this model cannot give a physically realistic response for $D_0 > 0.5$, since no wave length is possible in the softening regime. For the purely destabilized model ($l_s = 0, l_d = 1$) in the hardening regime a lower bound exists for the wave length, which governs the periodicity of the response (see the numerical analyses below). Similar to the classical model, no meaningful solutions can be obtained for the softening stage. On the other hand, the purely stabilized model does allow for a realistic solution in the softening regime, since a range of wave lengths have real phase velocities. However, these wave lengths are characterized by an upper bound, which can be found to be the size of the zone in which the strains tend to localize [1,12]. If both gradient terms are present at the same time with $l_s < l_d$, no meaningful solution can be obtained for damage levels $D_0 > 0.5$, although for damage levels close to one again real phase velocities are possible. When $l_s = l_d$, real phase
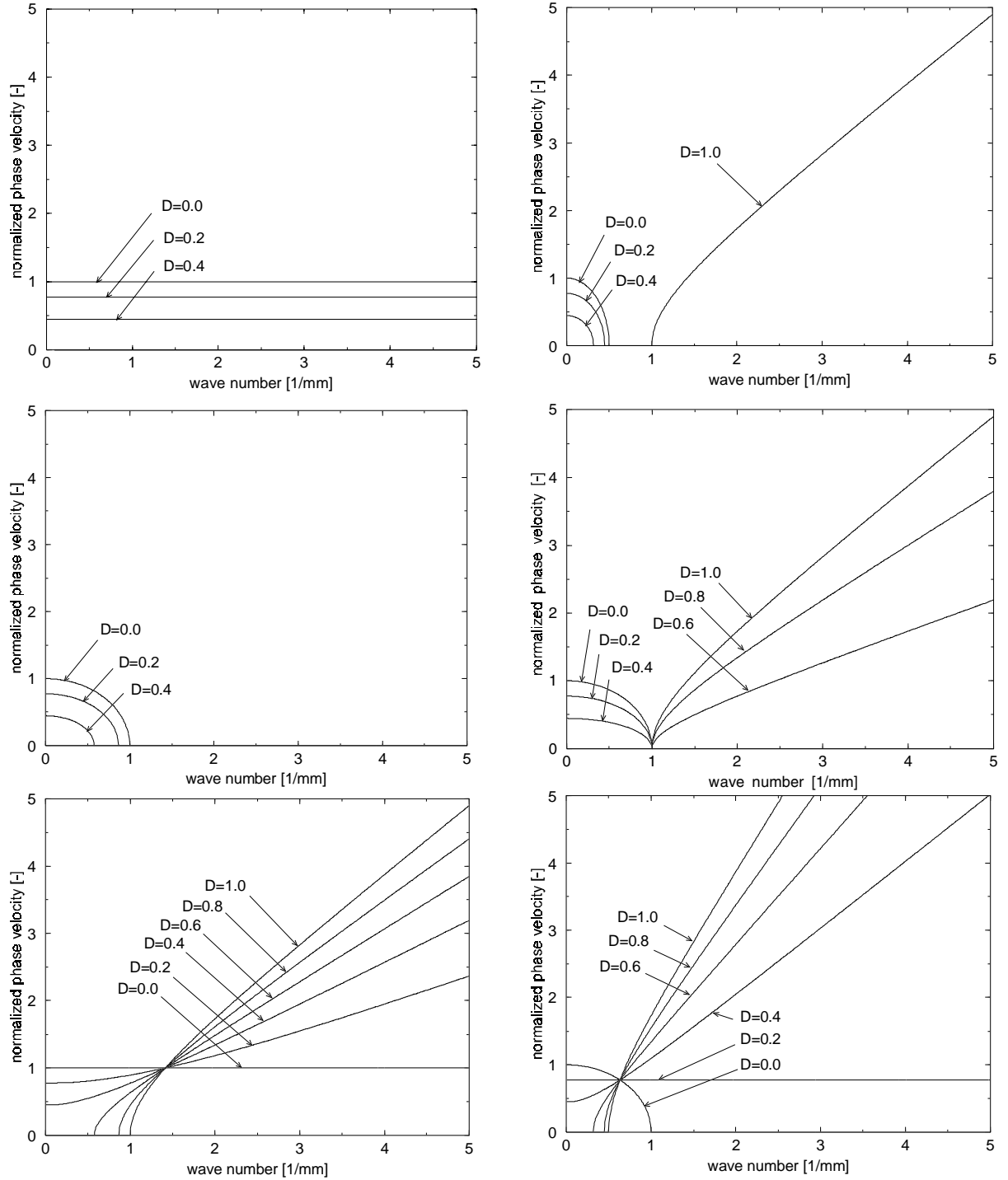
Fig. 1. Normalized phase velocity as a function of the wave number for different damage levels – $l_s=l_d=0$ (top left), $l_s=0$, $l_d=1$ (center left), $l_s=1$, $l_d=0$ (bottom left), $l_s=1$, $l_d=2$ (top right), $l_s=l_d=1$ (center right), $l_s=2$, $l_d=1$ (bottom right).

velocities are present during the entire loading process. In the hardening regime, a lower bound exists for the wave lengths of magnitude $2\pi l_s$. As soon as the softening regime is entered, this lower bound becomes an upper bound with exactly the same magnitude. Thus, around the damage level $D_0=0.5$ a sudden transition exists from the case where low-frequent waves can propagate while high-frequent waves cannot to the case where high-frequent waves can propagate while low-frequent waves cannot. This transition point appears to be difficult to pass in numerical analyses [16]. Finally, the model with $l_s > l_d \neq 0$ allows for real phase velocities during the complete loading process, while for low damage
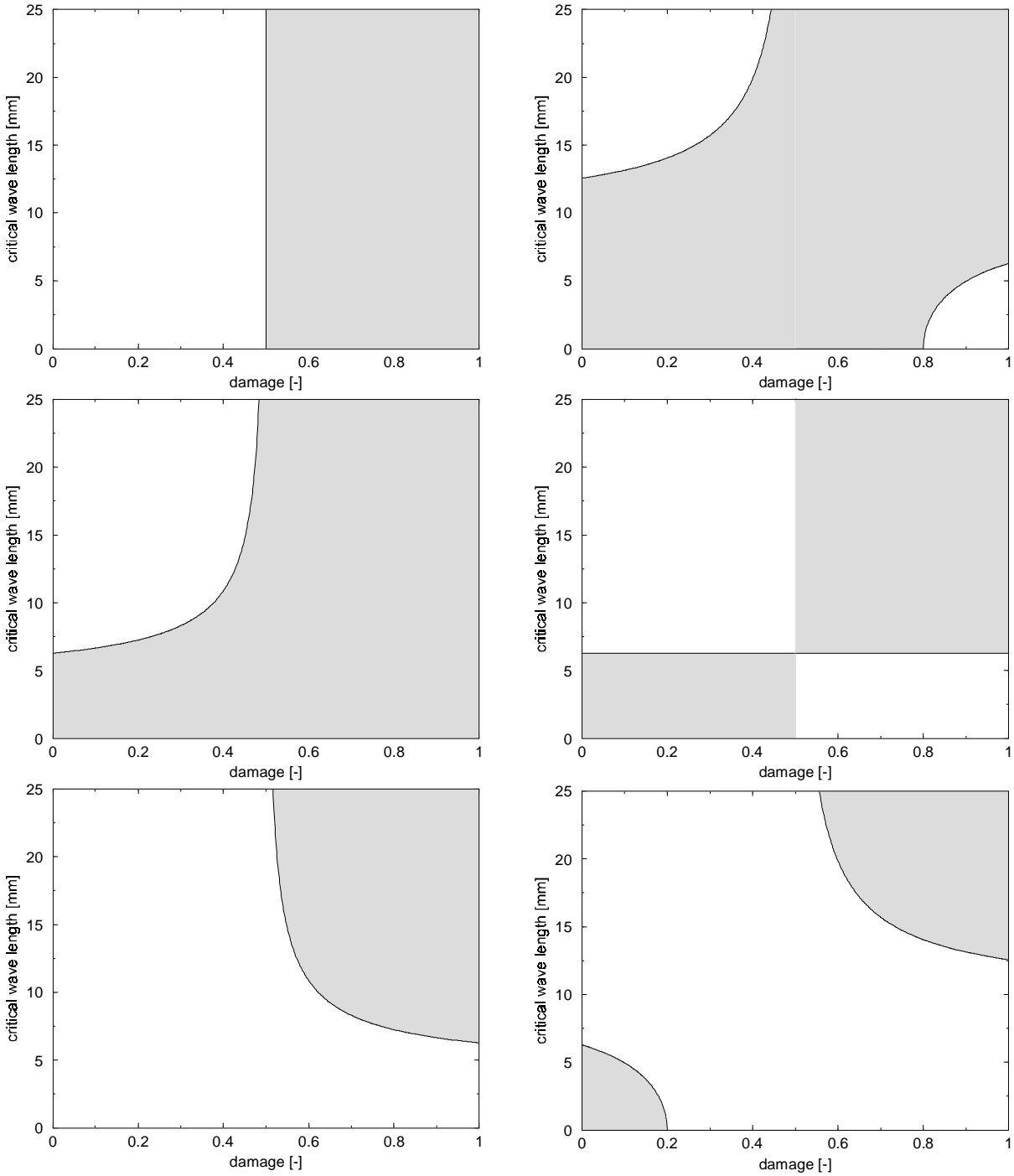
Fig. 2. Critical wave length as a function of the damage level, areas with imaginary phase velocities are shaded − $l_s = l_d = 0$ (top left), $l_s = 0$, $l_d = 1$ (center left), $l_s = 1$, $l_d = 0$ (bottom left), $l_s = 1$, $l_d = 2$ (top right), $l_s = l_d = 1$ (center right), $l_s = 2$, $l_d = 1$ (bottom right).

levels a lower bound exists for the wave lengths and for damage levels $D_0 > 0.5$ an upper bound exists.

In summary, the classical model, the purely de-stabilized model and the model with $l_d > l_s \neq 0$ are not able to give a meaningful solution in all loading stages. The model with $l_s = l_d \neq 0$ has a suspect transition point in its critical wave length curve. There-fore, the models that will be used in the numerical analyses are the purely stabilized model and the model with $l_s > l_d \neq 0$. Furthermore, to show the influence of the lower bound on the critical wave length also the purely destabilized model ($l_d \neq 0$, $l_s = 0$) is considered.
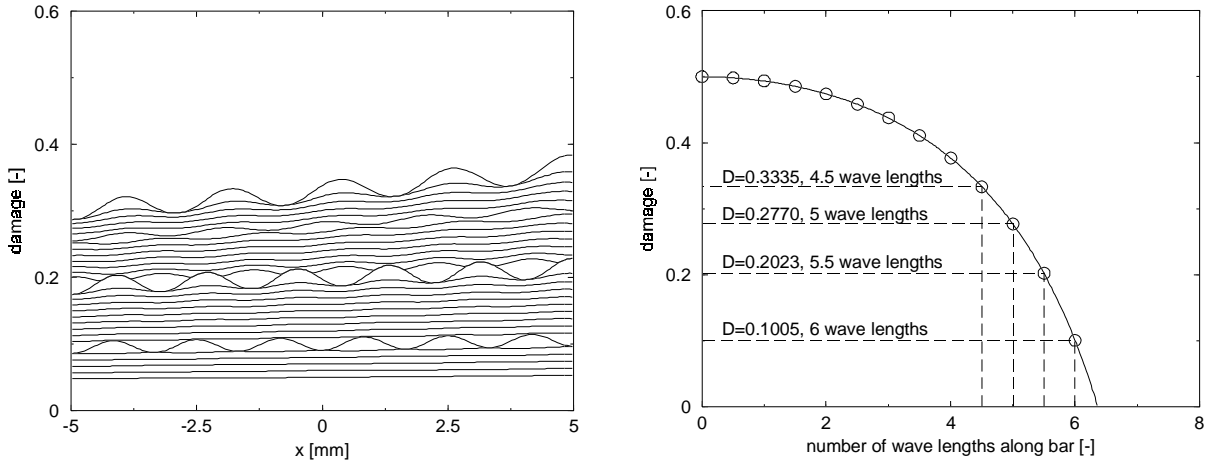
Fig. 3. Bar example – damage profiles (left) and unstable damage levels (right) for the case l_s=0, l_d=0.25 mm.

4. NUMERICAL SIMULATIONS

For the numerical analyses the Element-Free Galerkin (EFG) method is used [10,11]. The EFG method is a meshless discretisation method that formulates the shape functions entirely by means of a set of nodes, while no elements are needed. The EFG shape functions are easily formulated with an infinite order of continuity, which makes the EFG method a convenient tool for the testing of higher-order gradient models [12,13]. For the theoretical and implementational backgrounds the reader is referred to References [10-13]. We have used the EFG method to test the performance of the various higher-order gradient models in a nonlinear context.

In the numerical analyses a one-dimensional tensile bar is considered. The length of the bar is taken as L=10 mm while the cross section area is 1 mm². The material parameters are E=200 MPa and κ_u=0.01. The first model that is tested is the purely destabilized model with l_s=0 mm and l_d=0.25 mm. To trigger higher-order gradient activity the cross section area is changed such that it varies linearly from 1.05 mm² on the left end to 0.95 mm² on the right end. Displacement increments of 0.001 mm each are applied on the right end side. In Fig. 3 the damage profiles for consecutive load steps are plotted. While the response is more or less linear in most of the steps, in a number of increments a pattern of waves can be distinguished. Indeed, this corresponds to the analytical solution that has been found for the linear elastic case, see Eq. (4). The damage levels for which this periodic response occurs will be denoted as unstable damage levels as they have a deteriorating effect on the convergence

behaviour of the nonlinear analysis. Eventually, divergence occurs when the amplitude of the periodic response grows out of proportion. However, from Fig. 3, left, it can be seen that the frequency of the response changes from increment to increment. To understand this, the critical wave length curve of Fig. 2 must be studied. The unstable damage levels of Fig. 3 coincide with damage levels for which half the critical wave length fits an integer number of times into the bar length. Using $\lambda=2\pi/k$ and Eq. (11), a relation can be established between the number of wave lengths in the bar n and the damage level, i.e.

$$D_0 = \frac{1 - \dfrac{4\pi^2 n^2 l_d^2}{L^2}}{2 - \dfrac{4\pi^2 n^2 l_d^2}{L^2}}. \tag{12}$$

This relation is depicted in Fig. 3, right. The damage levels for which $2n$ is an integer correspond perfectly with those damage levels for which the numerical response shows a strong periodicity. Also the frequency of the response is in accordance with the theoretically derived numbers. Since these unstable damage levels follow each other more and more rapidly, the response has to switch more and more rapidly from one periodic mode to the next. This leads to impossible convergence requirements, so that it must be concluded that this model is unsuitable for use in static nonlinear analyses, even if no softening is present.

As an alternative, we study the model with l_s= 0.5 mm and l_d=0.25 mm, where real phase velocities exist for all damage levels. The same loading procedure as for the previous example has been
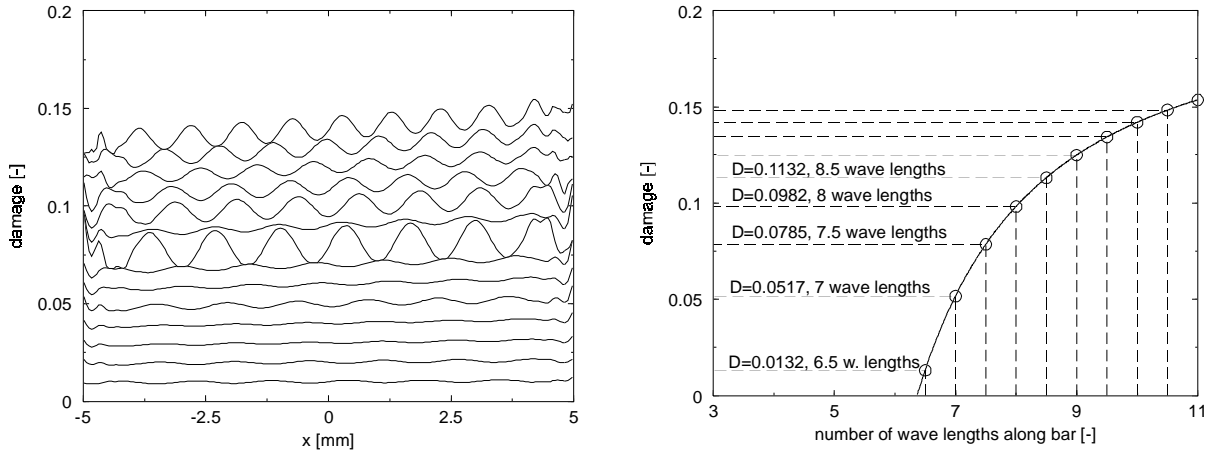
Fig. 4. Bar example – damage profiles (left) and unstable damage levels (right) for the case l_s=0.5, l_d=0.25 mm.

used, and the damage profiles for the different load steps are plotted in Fig. 4. Similar to the purely destabilized model, periodic responses are obtained for different increments, while again the periodicity of the response changes from step to step. In contrast to the purely destabilized model, the periodicity of the response now *increases* with increasing damage levels. However, again the critical wave length curve from Fig. 2 can be used to explain the periodicity of the response. Analogous to the above procedure, a relation can be derived between the damage level and the number of waves along the bar n as

$$D_0 = \frac{1 - \dfrac{4\pi^2 n^2 l_d^2}{L^2}}{2 - \dfrac{4\pi^2 n^2 l_d^2}{L^2} - \dfrac{4\pi^2 n^2 l_s^2}{L^2}}. \qquad (13)$$

If this number n is an integer or an integer plus a half, an unstable damage level results which becomes manifest through the large amplitude of the periodic response. Again, the theoretically derived unstable damage levels and the corresponding number of waves along the bar (see Fig. 4, right) correspond well to the numerical response (Fig. 4, left).

It has to be concluded that the stabilizing gradient term cannot be used to compensate for the divergent properties of the destabilizing term in the combined model. The only way in which a stable response can be obtained is to eliminate completely the destablizing effect by setting l_d=0. In this way, the purely stabilized model is retrieved. With this model, nonlinear analyses have been carried out. Since no lower bound on the wave length exists in the hardening traject, no periodicity is present in the response. Instead of a linearly varying cross section area, a cross section reduction of 10% has been taken in the central 0.5 mm of the bar. Fig. 5 shows the response of the bar. Since no unstable damage levels occur, the loading process can be continued until the end, i.e. until the load-carrying capacity has vanished completely and the damage has reached its ultimate value. The width of the damaging zone corresponds well to the prediction by the dispersion analysis. From Fig. 2 it can be seen that for D =1 the critical wave length of this model equals $2\pi l_s \approx$1.57 mm, which is in accordance with Fig. 5. Thus, the length scale l_s can be used to set the width of the damaging zone, by which also the energy dissipation can be set.

Remark 1. *It can be seen that the numerical behaviour of the purely destabilized model is in fact better than that of the combined stabilized/destabilized model. This seems strange at first, but it can be explained by how fast the unstable damage levels follow each other. In the purely destabilized model, the unstable damage levels converge towards a final value of 0.5 (see Figs. 2 and 3, right), while for the combined model as it is presented here they converge towards a final value of 0.2 (see Figs. 2 and 4, right). Thus, in the combined model divergence occurs at lower damage levels.*
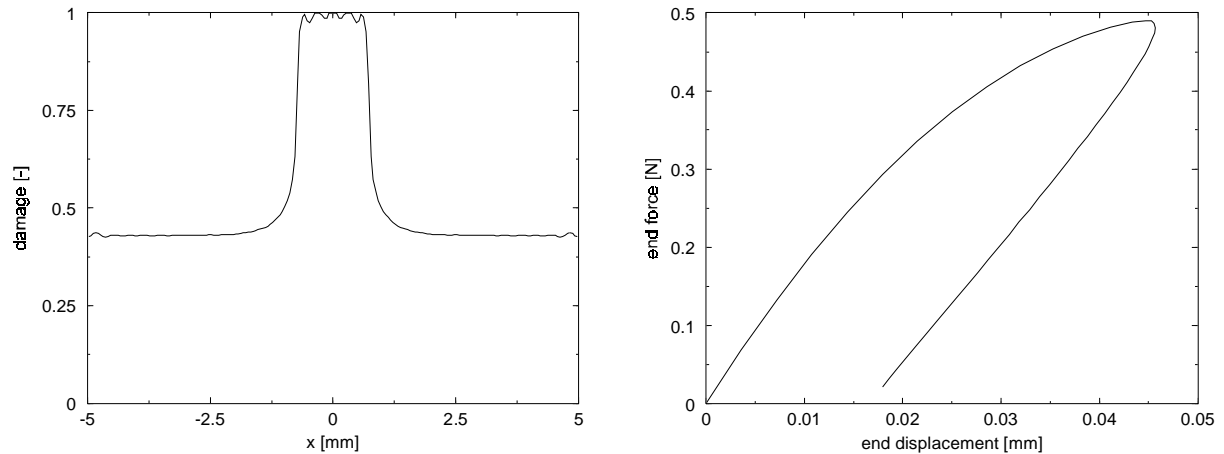
Fig. 5. Bar example – final damage profile (left) and global load-displacement diagram (right) for the case l_s=0.25, l_d=0 mm.

5. DISCUSSION

Enhanced continuum models in which second-order strain gradients are present have been studied from an analytical and a numerical point of view. A distinction is made between destabilizing gradients and stabilizing gradients, which is related to the sign of the gradient term in the constitutive relation. Specifically, a combined model is studied in which both effects have been incorporated. Dispersion analysis and numerical simulations with the Element-Free Galerkin method have been carried out to scrutinize the model characteristics. For the damage context that is taken, it appears that the destabilizing term deteriorates the model behaviour already in the hardening regime. This holds irrespective of whether the stabilizing term is present or not. Only when the destabilizing term is absent, a complete loading process can be carried out in which the load-carrying capacity reaches its ultimate zero-level. Thus, it can be concluded that the effects of a destabilizing second-order strain gradient cannot be compensated by the addition of a stabilizing second-order strain gradient. If the characteristics of the destabilizing terms (e.g. periodicity in the response) are desired in the continuum description, alternative ways must be found to compensate for the destabilizing effects. Under current investigation is the combination of second-order and fourth-order terms.

REFERENCES.

[1] L.J. Sluys, *Wave propagation,localosation and dispersion in softening solids, Dissertation* (Delft University of Technology,1992).

[2] R.H.J. Peerlings, R. de Borst, W.A.M. Brekelmans and J.H.P. de Vree // *International Journal for Numerical Methods in Engineering* **39** (1996) 3391.

[3] R. de Borst and H.-B. Muhlhaus // *International Journal for Numerical Methods in Engineering* **35** (1992) 521.

[4] J. Pamin, *Gradient-dependent plasticity in numerical simulation of localization phenomena, Dissertation* (Delft University of Technology,1994).

[5] D. Lasry and T. Belytschko // *International Journal for Solid and Structures* **24** (1988) 581.

[6] H.-B. Muhlhaus and F. Oka // *International Journal for Solid and Structures* **33** (1996) 271.

[7] C.S. Chang and J.Gao // *International Journal for Solid and Structures* **32** (1995) 2279.

[8] A.S.J. Suiker, C.S. Chang and R. de Borst // *Acta Mechanica,* accepted for publication.

[9] H. Askes, A.S.J. Suiker and L.J. Sluys, *Dispersion and numerical analysis of higher order gradient models in homogenized and regularized media, Tech. Report 03.21.1.31.07* (T.U. Delft, 1999).

[10] T. Belytchko, Y.Y. Lu and L. Gu // *International Journal for Numerical Methods in Engineering* **37** (1994) 229.

[11] T. Belytchko, Y. Krongauz, D. Organ, M. Fleming and P. Krysl // *Computer Methods in Applied Mechanics and Engineering* **139** (1996) 3.

[12] H. Askes, J. Pamin and R. de Borst // *International Journal for Numerical Methods in Engineering* **49** (2000) 811*.*

[13] J. Pamin, H. Askes and R. de Borst, In: *Proc. European Conference on Computational Mechanics Solids, Structures and Coupled Problems in Engineering*, ed. by W. Wunderlich, 1999.

[14] Z.P. Bazant and G. Pijaudier-Cabot // *ASCE Journal of Engineering Mechanics* **115** (1989) 755.

[15] H.-B. Muhlhaus I. Vardoulakis // *Geotechnique* **37** (1987) 271.

[16] A.S.J. Suiker, H. Askes and L.J. Sluys, In: *Proc. European Congress on Computational Methods in Applied Sciences and Engineering*, 2000.